Debonding Detection in the Grouted Joints of Precast Concrete Shear Walls Using Impact-Echo Method

Yun-Lin Liu[a], Zhihao Liu[a], Siu-Kai Lai[b*], Li-Zi Luo[b] and Jian-Guo Dai[b*]

[a] School of Civil Engineering, Anhui Jianzhu University, Hefei, China

[b] Department of Civil and Environmental Engineering, The Hong Kong Polytechnic University, Hong Kong, China

Corresponding authors: S.K. Lai (sk.lai@polyu.edu.hk); J.G. Dai (cejgdai@polyu.edu.hk)

Abstract: A grout layer between precast concrete components in an assembly structure is required to bear high axial loads and withstand significant shear forces during earthquakes. Since the grout layer usually exists in a narrow space, examining the quality of the layer, particularly detecting debonding at the interface, is a difficult task. However, a debonding defect at the interface is likely to significantly reduce the safety performance of structures. To address this problem, this paper presents a combined experimental and numerical study to detect the interfacial debonding based on the impact-echo theory. Two precast concrete shear walls assembled in a structure were tested by the impact-echo method based on two different boundaries. It is shown that the thickness frequencies near a free boundary are considerably lower than those near a fixed boundary, and the boundary effect disappears when the impact position is far away from the free boundary or the fixed boundary. Such characteristics can be used to identify a debonded layer (i.e., approaching the free boundary) in the grouted joint. A blind in-situ test was also conducted to validate the effectiveness of the proposed impact echo method in detecting debonded layers.

Keywords: Precast concrete structures; Impact-echo method; Shear wall; Grout layer; Debonding detection

1. Introduction

Precast concrete structures made up of components prefabricated in factories have gained worldwide popularity. Ready-made loose components such as precast concrete shear walls, columns, beams and slabs are installed on site to form precast structures. The joints between the components, particularly the loadbearing ones (e.g., precast walls and columns) play an important role in maintaining the safety performance of structures. The gap in the joints which is required for alignment is usually filled with a dry pack grout [1] or a grout layer (see Figure 1) to bear high axial pressure and horizontal shear forces. Debonding defects at the interface between the grout layer and the adjacent member (see Figure 2) might be generated by the grout shrinkage or improper construction procedures, thereby compromising the overall performance of structures. Therefore, it is critically important to inspect and evaluate debonding at the interface in order to guarantee the safety and serviceability performance of precast structures.

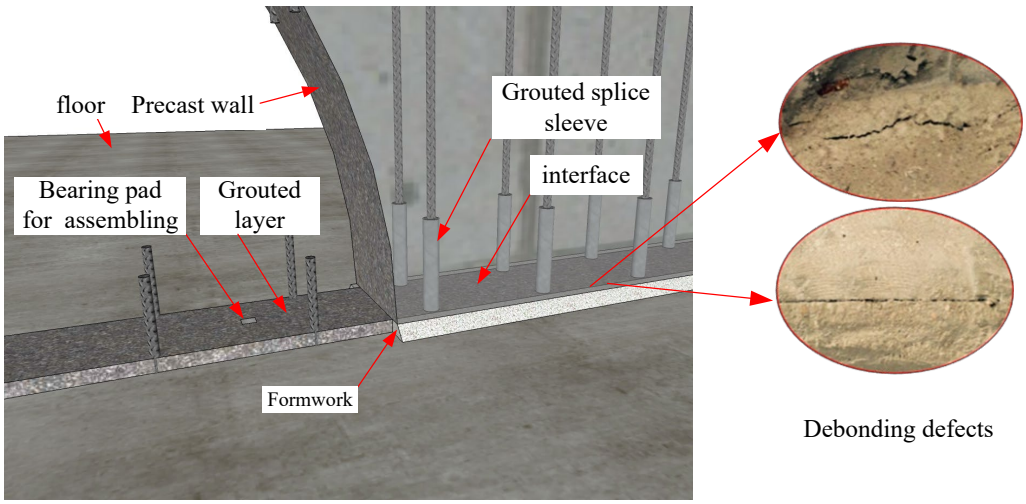

Figure 1. The connection details of a precast concrete shear wall

Core sampling is a time-consuming and costly method for evaluating the internal conditions of concrete, and in fact it is not applicable for the above-mentioned situation. On the other hand, nondestructive testing (NDT) methods are appreciated for its cost-effectiveness and avoidance of damage. There are many kinds of NDT methods such as the conventional ultrasonic testing method, the ground penetrating radar method and the impact-echo (IE) method, which are often used to

inspect the conditions of concrete structures [2-5]. However, most of them cannot be operated in a narrow space and no application was reported for the working condition in the joint area of precast concrete shear walls, which is the focus of the present study.

The IE method is one of the latest techniques that uses the principle of stress wave propagation induced by a short-term mechanical impact to rapidly detect voids or debonding in concrete elements [5, 6]. This method has been successfully adopted to detect flaws in concrete beams and columns [7], concrete blocks [8], prestressed concrete slabs [9], epoxy–concrete interfaces [10], bridge decks [11] and I-girders [12], voids in grouted tunnel lining [13] and voids in the grouted ducts of prestressed concrete structures [14-17].

Flaws in concrete structures usually orient approximately in parallel to the impact surface. However, the orientation of the debonded interface of precast structures in this study is perpendicular to the surface (see Figure 2a), which makes the impact-echo response far more complicated. This paper thus aims to investigate the impact-echo responses of precast panels near the interface and proposes a method to detect debonding between the grout layer and the adjacent precast component.

2. Research Methods

2.1. Theoretical background

IE is a nondestructive testing method based on analyzing the characteristics of reflected transient stress waves especially the primary wave (P-wave) at the surface near the impact point [5]. The stress wave stimulated by an elastic impact (usually using a small steel ball) propagates in solid objects mainly in the ways of P-wave, S-wave, and R-wave [5]. The P-wave is a pressure wave and travels faster than the others in solid structures. It will be reflected when encountering

external boundaries or internal defects such as voids, cracks or debonding, which can be evaluated through monitoring the surface displacements generated by the reflected P-wave using an acceleration transducer located close to the impact point [5]. The frequency spectrum of the recorded time-displacement signal can be obtained by the Fast Fourier Transform (FFT) technique. The frequencies with amplitude peaks in the resulting amplitude spectrum are typically used to estimate the thickness of objects and the existence of internal flaws [5].

The frequency with a peak amplitude in the obtained spectrum represents the dominant frequency in the waveform. This dominant frequency, also known as the thickness frequency, can be estimated as [18]

$$f = \frac{\beta K}{n}\frac{C_p}{T} \tag{1}$$

where

$$C_p = \sqrt{\frac{E(1-\nu)}{\rho(1+\nu)(1-2\nu)}} \tag{2}$$

K is a geometric correction factor that is determined by the geometrical shape of the structure [18]; T is the sectional thickness of structure; n is a constant factor either equal to 2 or 4 depending on the acoustic impedance [18]; β is a correction factor, the value is 0.96 [5] in a plate-like structure or 0.95 [19] while in a bar-like structure such as concrete beam and column, the value of β varies from 0.75 to 0.96 with the aspect ratios of the cross-section [5, 18]; C_p is the P-wave speed, where E, ρ, and ν are the elastic modulus, density, and Poisson's ratio of the test object, respectively. In this study, K, β, and n are equal to 1.0, 0.96, and 2.0 for the precast panels, respectively [5]. The above values of β have been adopted by the ASTM standards and thus the engineering practice. For plate-like structures, however, the impact echo frequency has been fully explained based on Lamb wave theory in plates [20-24]. The actual impact echo resonance is a superposition of both P- and S-waves propagating in both directions along the plate [23, 24]. The theoretical β factor for the plate-like structures is only dependent on the Poisson's ratio [22].

Unlike plate-like and bar-like structures, the precast panels near the interface (see Figure 2) subject to a transverse impact have more profound impact responses for complex boundaries. If the grout layer is tightly attached with the wall, the stress wave passes the interface and the front P-wave is directly reflected from the opposite surface (see Figure 2a). On the other hand, if there is a debonding defect at the interface, the wave propagation pattern differs significantly from that in a sound interface. This is because the debonding defect is a concrete/air interface that reflects the stress wave to propagate outward from the boundary (i.e., the debonded interface, see Figure 2b). This condition coincides with the contour vibrations of a thin rectangular plate [25] and the edge resonance of a plate in the previous studies [26, 27]. In the present work, the impact responses for the above-mentioned two different situations are investigated to compare various spectral responses, so that the debonding interface between the grout layer and the adjacent precast component can be recognized.

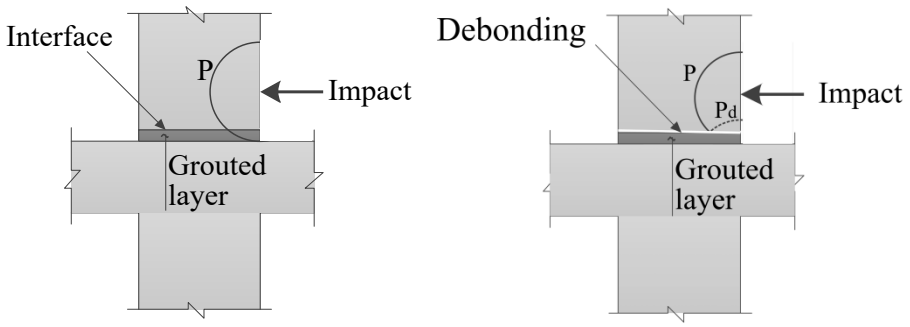

(a) Tight interface (b) Debonded interface

Figure 2. Two different propagating patterns of stress waves

2.2. IE test method

An IE test facility developed by Sichuan Central Inspection Technology Co. Ltd. was adopted for the experimental test. This facility has four primary components, including an impactor with a steel ball, an accelerometer with a model number of S21C (a frequency range up to 15 kHz), a signal amplifier, and a laptop with data processing system (see Figure 3). Selecting a proper impactor whose diameter exhibits a linear function of the contact time (t_c) with the tested object is

crucial to achieve a frequency range matching with the frequencies of the generated stress wave. The maximum frequency of a wave with a sufficient fluctuation amplitude is approximately $1.25/t_c$ [5]. The impact force and the contact time have a relationship defined as a half-cycle sinusoidal function [5]. An impactor with a 6-mm steel sphere which has a contact time of approximately 25 μs with the concrete [5] was adopted in the present tests. By positioning the receiver next to the impact source, signals were detected to be proportional to the vertical surface acceleration. The waveforms captured by the transducer were stored in a portable computer-based data-acquisition system and exported for signal processing and analysis. As a result, the waveform consisted of 4096 data and had a time interval of 2 μs, which can generate a spectral resolution of 0.122 kHz.

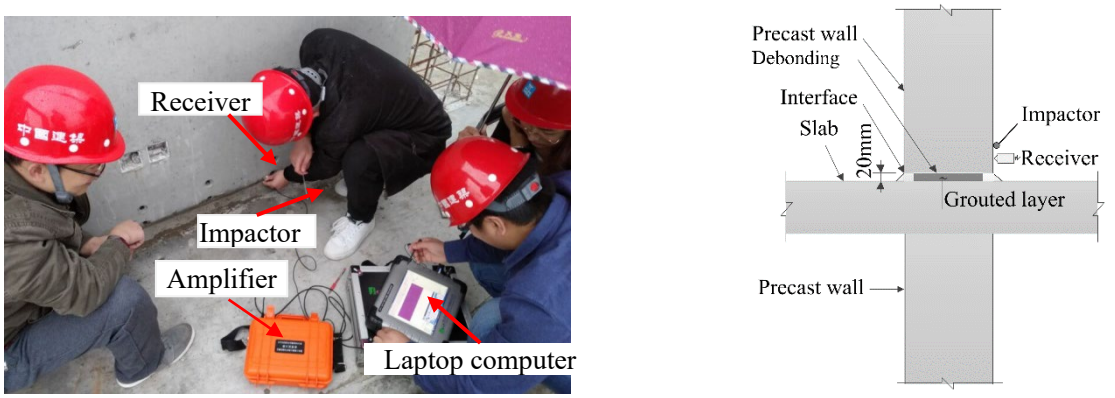

(a) Impact-echo test on site (b) Cross section at the test location

Figure 3. Impact-echo test

A precast wall was assembled on site to investigate two different boundaries. As shown in Figure 4, the wall is 2900 mm in height, 3500 mm in width and 200 mm in thickness, respectively. The free boundary is defined in Figure 4a to simulate a typical concrete/air interface and the fixed boundary was formed at a well grouted joint space (see Figure 4b). To conduct the in-situ test, 10 test lines in the direction parallel to the free and fixed boundaries were marked with a spacing of 1cm (see Figures 4a and 4b). The results of the testing points (numbered from 1 to 9 and from 10 to 18) were measured by different technicians in order to rule out of human errors.

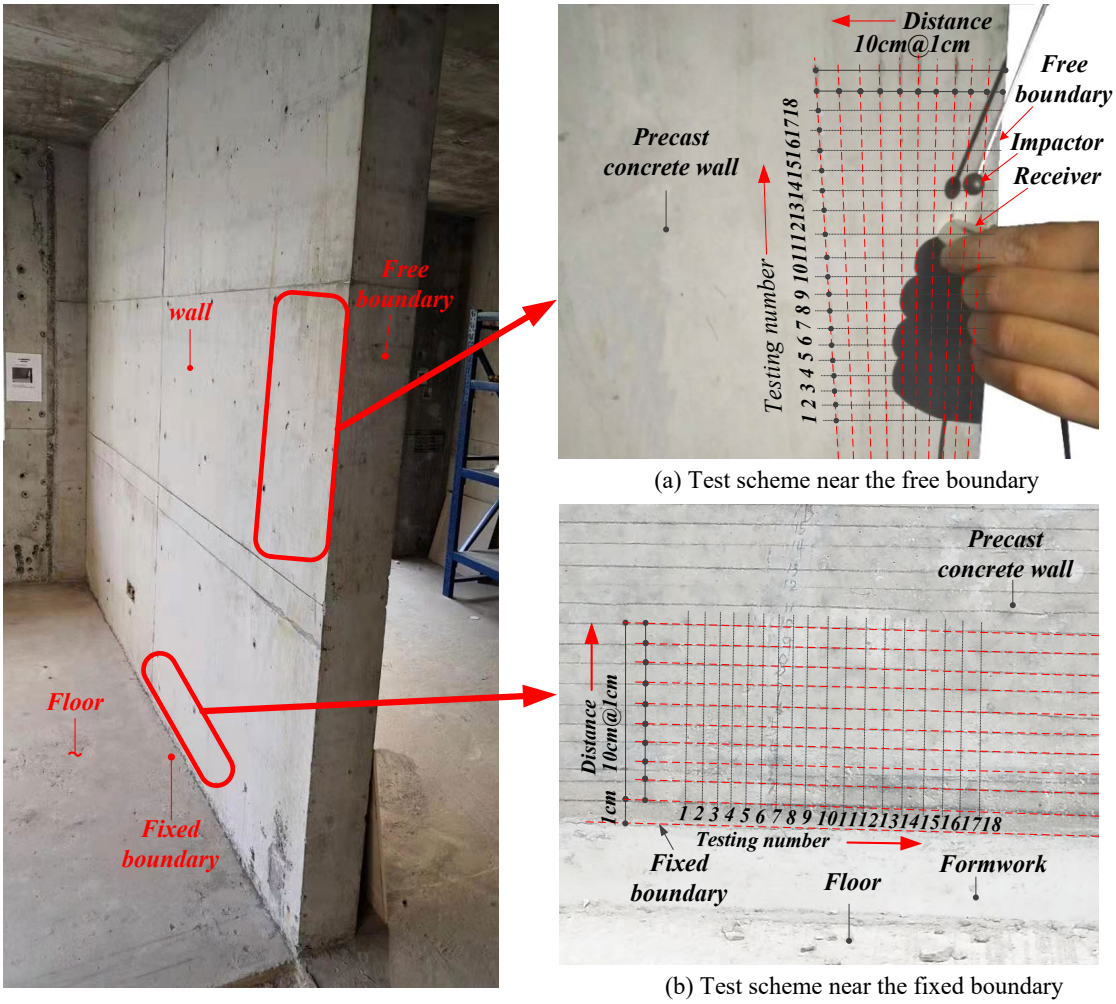

(a) Test scheme near the free boundary

(b) Test scheme near the fixed boundary

Figure 4. Experimental test scheme

2.3. Numerical analysis

Three-dimensional models (C3D8R element in ABAQUS) subject to a transverse impact force were developed here to study the patterns of IE responses by varying distance (d) between the impact point and the free boundary. The interface contact type was set to be "bond". The thickness of the shear wall was 200 mm. Figure 5 illustrates the dimensions of the numerical models, in which the 8-node linear brick element was adopted and the reinforcement of the panels was ignored as they have little effect on the response frequencies [5]. A 5-mm meshing size was used for the 8-node linear brick element in accordance with a convergence study. The relationship between the impact force and the contact time used in the numerical model followed a half sine curve and the contact time (t_c) of the impact was 25 μs.

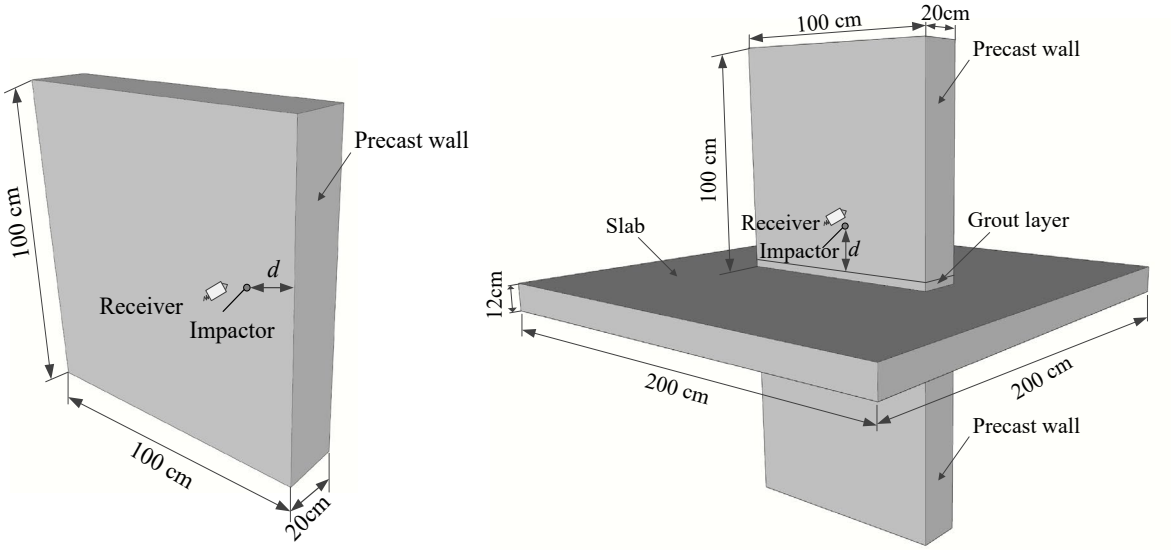

(a) Near the free boundary (b) Near the fixed boundary

Figure 5. Configuration of numerical models

The material properties of concrete used in the numerical models are summarized in Table 1, the value of C_p can be calculated by Eq. (2).

Table 1. Material properties

Parameter	Concrete	Grout material
Mass density, ρ (kg/m^3)	2440	2400
Young's Modulus, E (GPa)	44.0	30.6
Poisson's ratio, v	0.2	0.2
P-wave speed , C_p (m/s)	4476.2	3763.9

3. Results and Discussion

3.1. Test results

Figure 6 shows the impact response frequencies varying with different test numbers and locations from the boundaries. As shown in Figure 6a, the test results remained stable at the same distance from the free boundary regardless of the testing points and frequency change when the distance to the boundary increases up to around 6 cm. Unlike the responses near the free boundary, there are some random shifts in the IE frequencies near the fixed boundary (see Figure 6b) because

of the complexity around the boundary. However, the values of frequencies are around the control frequency of 10.620 kHz which is obtained from the center of the precast concrete shear wall, where the boundary effect is removed.

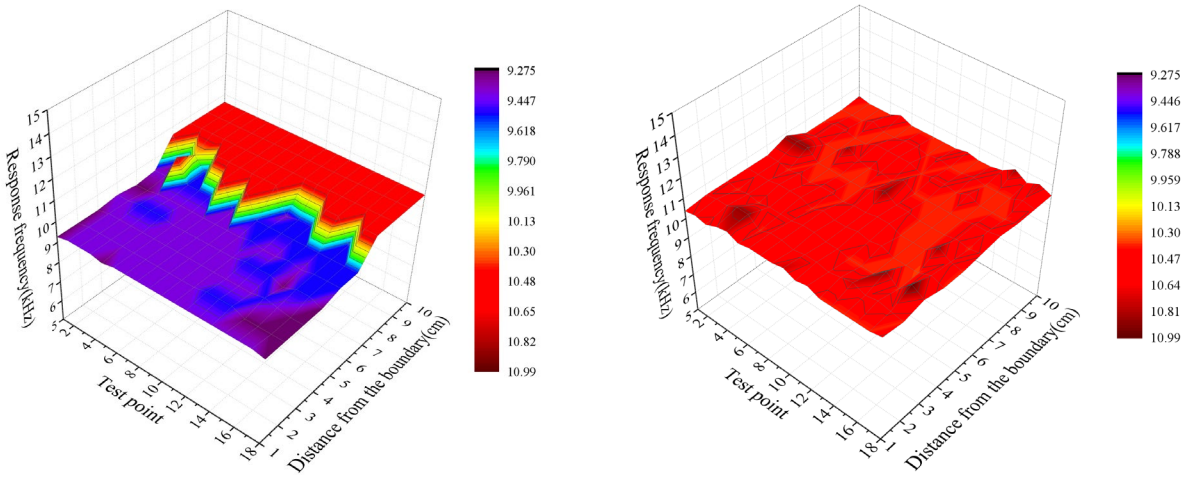

(a) (b)

Figure 6. 3D frequency contours of the test results: (a) IE responses near the free boundary; and (b) IE responses near the fixed boundary

The mean response frequency values are listed in Table 2. In the case near the free boundary, the frequency values fluctuate around 9.385 kHz when the distance between the impact point and the free boundary is less than 4 cm. When the distance increases further to 8 cm, the predominant peak frequency is stabilized at a higher value of 10.620 kHz which is close to the fundamental thickness frequency of the precast concrete shear wall (i.e., 10.742 kHz) as calculated by Eq.(1). However, when the distance increases from 4 cm to 8 cm, the predominant peak frequencies increase with the distance. In the case of responses near the fixed boundary, the frequencies declines slightly with the increase of the distance while overall the values approach the fundamental thickness frequency of 10.742 kHz. Figure 7 illustrates the tendency of the response frequencies near the two different boundaries for better comparison.

195 **Table 2.** Experimental frequency responses

Distance from the boundary (d, cm)	1	2	3	4	5	6	7	8	9	10
Frequency near the free boundary (kHz)	9.379	9.385	9.385	9.440	9.419	9.684	10.206	10.620	10.620	10.620
Frequency near the fixed boundary (kHz)	10.511	10.592	10.525	10.511	10.484	10.525	10.470	10.477	10.437	10.470

196

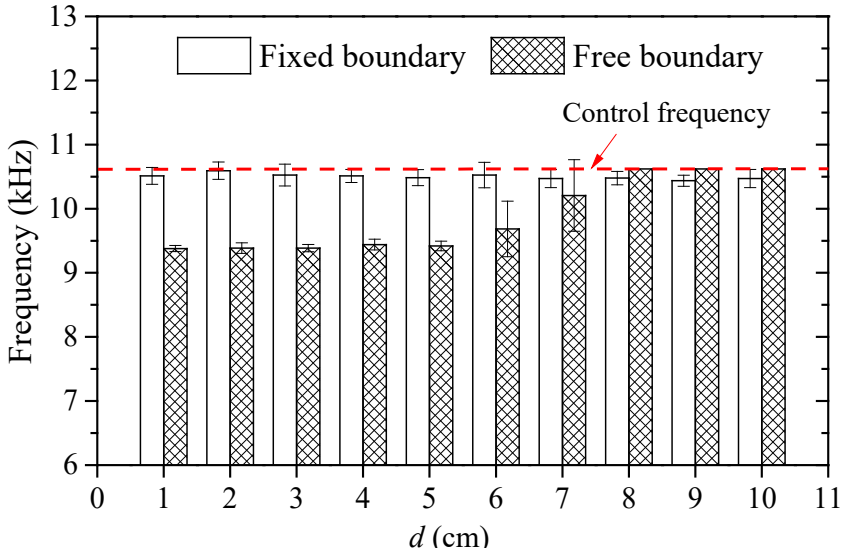

197

198 **Figure 7.** Comparison of testing results between free and fixed boundary

199 3.2. Numerical results

200 Table 3 shows the numerical simulation results. In the case of values near the free boundary,
201 the predominant peak frequency is about 9.763 kHz when the distance between the impact point
202 and the boundary varies between 1 cm and 4 cm. When the distance exceeds 6 cm, the predominant
203 peak frequency tends to be stabilized at 10.739 kHz which is in reasonable agreement with the
204 calculated fundamental thickness frequency of 10.742 kHz. This phenomenon can be explained by
205 the variation of spectrum with distance near the free boundary, as shown in Figures 8a and 8b,
206 which illustrate the spectra of frequencies predicted at the locations of 5 cm and 6 cm from the
207 free boundary, respectively. When the distance is 5 cm, the predominant peak frequency of 9.763
208 kHz appears accompanying the frequency of 10.739 kHz, while the distance is increased to 6 cm,

the frequency of 10.739 kHz becomes dominant. Indeed, the propagation of stress wave is affected by boundary conditions due to the interference between the incident and diffracted modes [27].

Table 3. Simulated frequency responses

Distance from the boundary (d, cm)	1	2	3	4	5	6	7	8	9	10
Frequency near the free boundary (kHz)	9.763	9.763	9.763	9.763	10.251	10.251	10.739	10.739	10.739	10.739
Frequency near the fixed boundary (kHz)	13.546	13.546	13.546	13.546	12.508	12.508	11.471	11.471	10.861	10.861

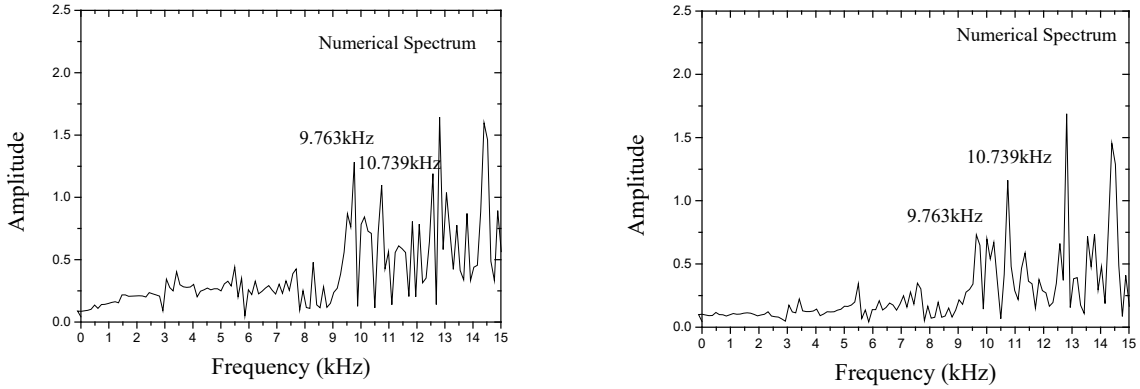

(a) d = 5 cm (b) d = 6 cm

Figure 8. Numerical spectrum near the free boundary

In the case near the fixed boundary in Table 3, the predicted response frequencies at all the locations were larger than the fundamental thickness frequency of 10.742 kHz. When the distance between the impact point and the fixed boundary was within 5 cm, the predominant peak frequency appeared at 13.546 kHz. Beyond that the frequency of 11.471 kHz became dominant. Figures 9a and 9b illustrate the spectra of frequencies predicted at the locations of 5 cm and 6 cm from the fixed boundary, respectively.

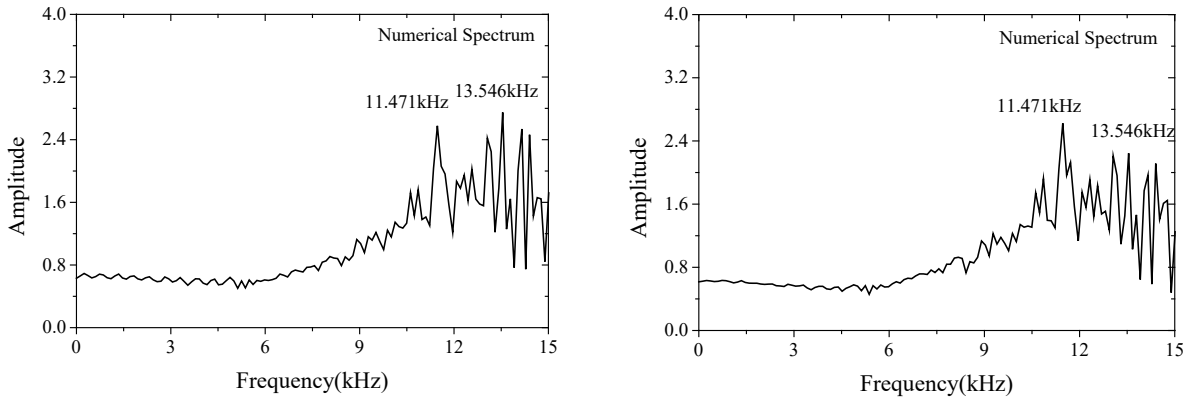

(a) d = 5 cm (b) d = 6 cm

Figure 9. Numerical spectrum near the fixed boundary

222

223 3.3. Discussion

224 Overall, the experimental results near the free boundary are in reasonable agreement with the
225 numerical ones (see Table 4) although there are some gaps (see Figure 10a) for the locations
226 between 5 cm and 8 cm. Both numerical and experimental results demonstrate that the existence
227 of free boundary may significantly affect the frequency response within the distance of 5 cm from
228 the boundary. The IE response characteristic near the free boundary is between those of a bar-like
229 structure and a plate-like structure, since the shape factor β near the free boundary can be obtained
230 as 0.897 in the numerical study and about 0.883 in the experimental test, both values fall within
231 the range of 0.87 to 0.96 [5]. This abrupt frequency variation phenomenon can also be interpreted
232 by the generation of zero-group-velocity (ZGV) and edge modes [25, 26]. When the distance from
233 the boundary comes to the thickness of the plate, the amplitude of the ZGV resonance vanishes
234 while the edge mode resonance appears at a lower frequency [25, 26].

235

Table 4. Summary of the experimental and numerical frequency responses

Distance from the boundary (d, cm)		1	2	3	4	5	6	7	8	9	10
Frequency near the free boundary (kHz)	Experimental results	9.379	9.385	9.385	9.440	9.419	9.684	10.206	10.620	10.620	10.620
	Numerical results	9.763	9.763	9.763	9.763	10.251	10.251	10.739	10.739	10.739	10.739
Frequency near the fixed boundary (kHz)	Experimental results	10.511	10.592	10.525	10.511	10.484	10.525	10.470	10.477	10.437	10.470
	Numerical results	13.546	13.546	13.546	13.546	12.508	12.508	11.471	11.471	10.861	10.861

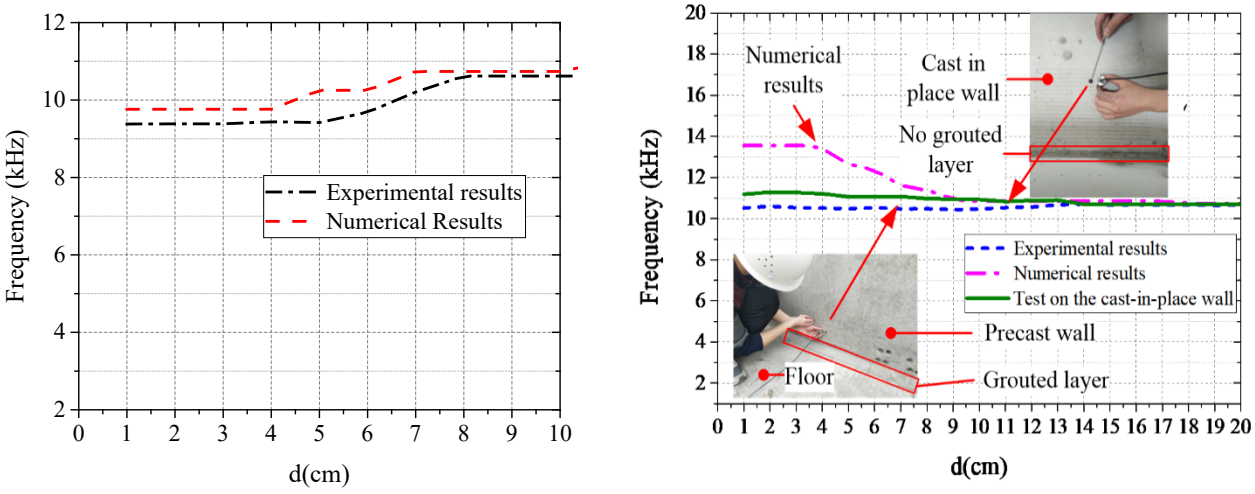

Figure 10. Comparison of numerical and experimental frequency responses: (a) frequency responses near the free boundary; and (b) frequency responses near the fixed boundary

Figure 10b shows a comparison between experimental and numerical results in terms of the frequency responses at different positions from the fixed boundary. It is seen that, the experimental frequencies tend to converge to a level of 10.525 kHz beyond 14 cm from the fixed boundary, which is approximately the same as the predicted control frequency (i.e., 10.620 kHz). However, a quite big difference exists between the experimental and numerical results within a relatively short distance (i.e., about 4 cm) in the fixed boundary case. It is probably due to the real boundary condition of the precast shear wall does not fully satisfy the fixed boundary condition adopted by the numerical model whose stiffness is larger than the actual stiffness. Therefore, to validate such

an assumption, another piece of a cast-in-place shear wall (i.e., no grouted layer joint, as shown in Figure 10b) was prepared and the measured experimental frequencies within the distance of 20 cm from the fixed boundary are also presented in Figure 10b for comparison. It is clearly seen that experimental frequencies of the cast-in-place wall which is also higher than the control frequency decrease with the distance from fixed boundary until 14 cm, In other words, it is possible to judge whether there is a debonding defect in the grouted joint using the IE method through observing the change of patterns of response frequencies with the distance from the possible debonded layer, particularly within a distance of 15 cm. An obvious jump of the frequency from a lower value to a higher value (e.g., Figure 10a) may reveal the existence of a free boundary, i.e., a debonded layer.

4. Blind Study on Site

4.1. Procedures

Field studies were conducted on two precast concrete shear walls (denoted as A and B) to verify the effectiveness of the proposed impact-echo scenario in detecting the debonded layer. The test was performed as a blind study in which the operators did not know in advance the grouting conditions of the two specimens. As the above analysis has revealed, the frequency will shift to a lower value due to the influence of free boundary when the distance between the impact point and the free boundary is within 6 cm. This means the existence of debonding in the grout layer can be found through the IE method because it may introduce a free boundary effect. To realize this, firstly it is important to select a suitable impact distance. In this study, the distance between the impact point and the precast concrete shear wall's boundary was controlled at 3 cm (see Figure 11). The reference control frequency was obtained by impacting the center of the solid precast wall panels.

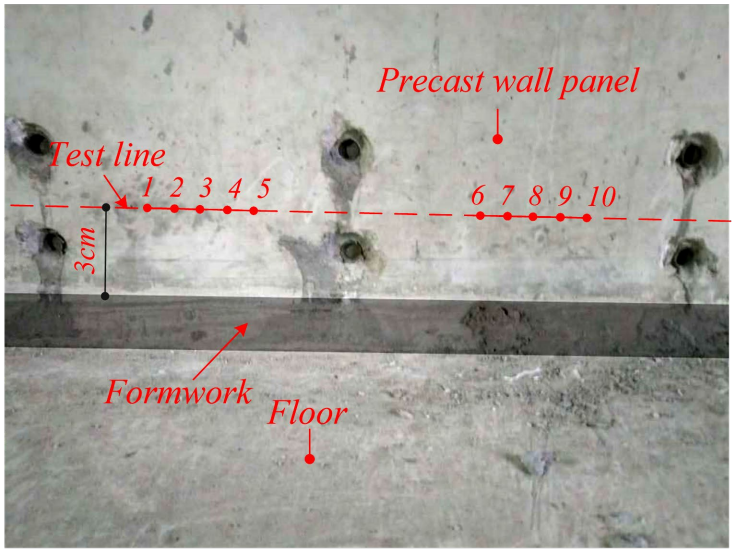

Figure 11. Test line for an in-situ joint

4.2. Results of IE Test

Figure 12 shows the test results of specimen A and specimen B. Test numbers 11 to 13 were located around the center of each wall, through which the control frequency was found to be 10.375 kHz and 10.253 kHz, respectively. The test frequencies of other 10 measurement points on the specimen A were almost the same as its control frequency while the frequency responses of the specimen B were obviously lower than the control value, indicating the existence of debonding in the grout layer, i.e., a free boundary at the bottom of the shear wall. As shown in Figure 12, the presence of an interfacial debonding was discovered after the grouted layer was chiseled.

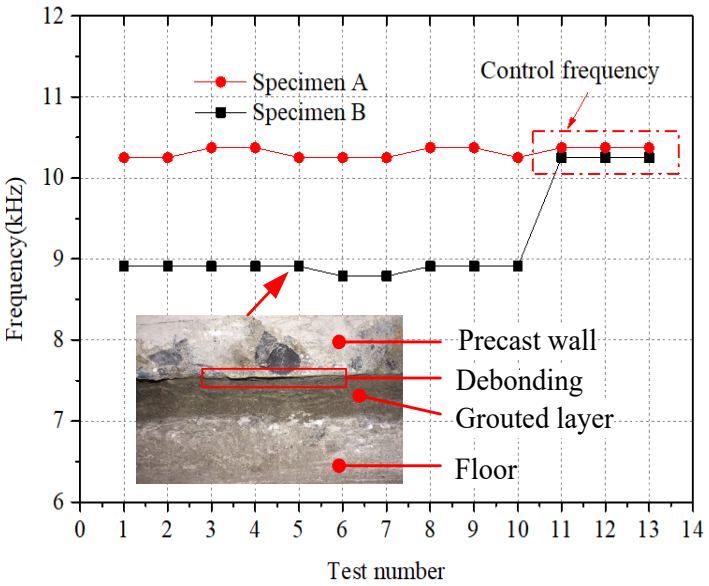

Figure 12. Experimental results in the blind test

Figures 13 and 14 illustrate the typical acceleration waveforms and frequency spectra obtained from the tests on specimen A and specimen B, respectively. The main duration time and its corresponding frequency are labeled in the figures. As shown in Figure 13, the first wave arrived was the R-wave [5]. The elapsed time t_1 (about 0.096 ms) is the distance where the P-wave traveled, corresponding to the frequency of 10.375 kHz. The large amplitude peak at 2.808 kHz, corresponding to the duration time of t_2 (about 0.356 ms), was excited by the flexural vibration of the wall section [5]. In Figure 14, the frequency values of the second peak are different, implying that there was an interfacial defect in the specimen. Indeed, the project workers verified that specimen A was carefully grouted while specimen B was only partially grouted. Therefore, the proposed IE scheme proved its success in detecting debonding adjacent to the grout layer.

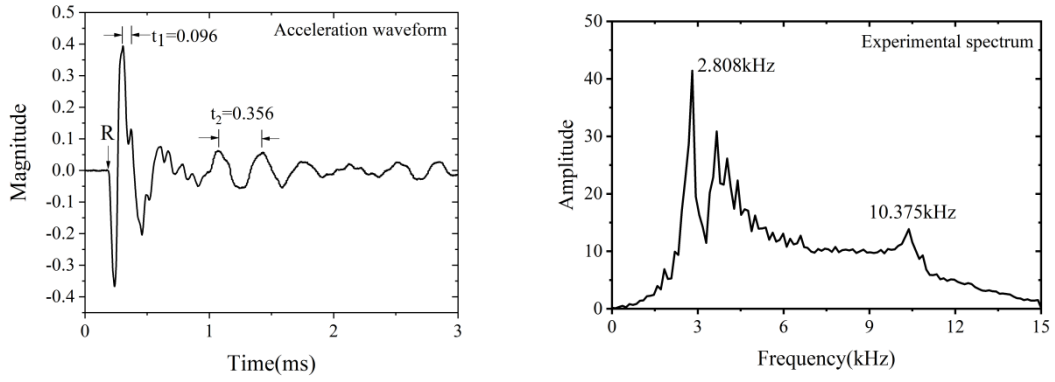

(a) d = 3 cm

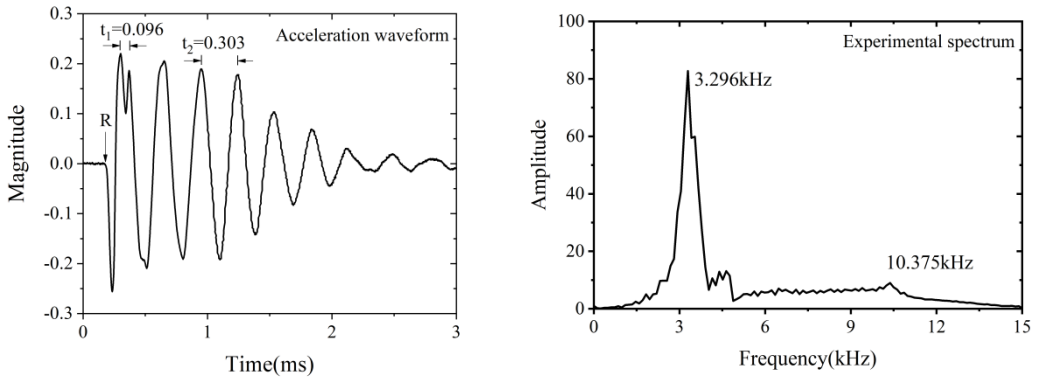

(b) Center of the wall

Figure 13. Acceleration waveform and frequency spectrum of specimen A

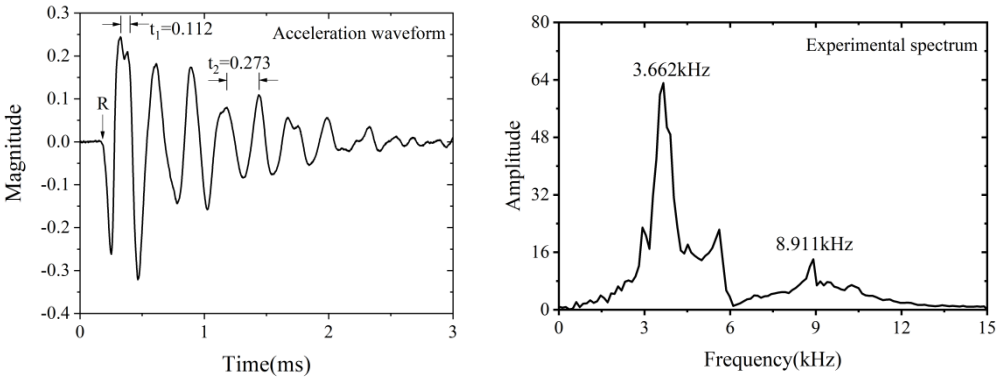

(a) d = 3 cm

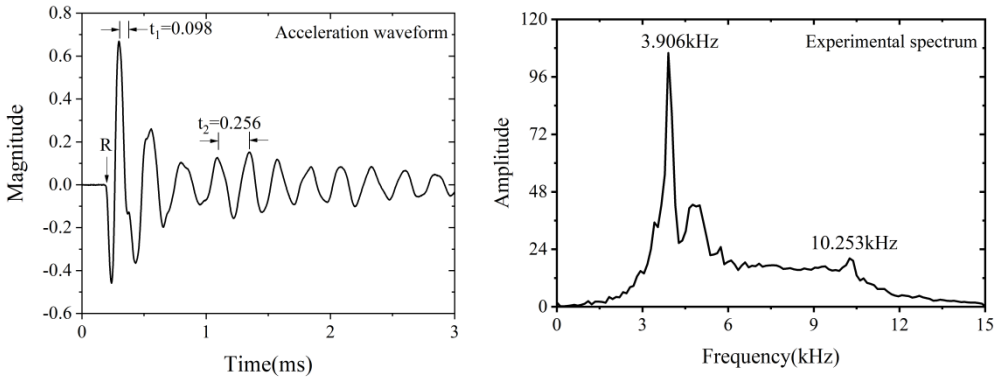

(b) Center of the wall

Figure 14. Acceleration waveform and frequency spectrum of specimen B

5. Conclusions

A detailed investigation into the typical impact-echo responses near the free and fixed boundaries of precast concrete shear walls has been conducted. Through a field study conducted on two precast concrete panel wall joints containing a perfect and a deficient grout layer, respectively, the effectiveness of the impact-echo method in detecting debonding at the joint interface has been demonstrated.

The experimental and numerical tests showed that, if there is debonding between the grout layer and the adjacent precast concrete shear wall, the IE test results are apparently influenced by the free boundary condition. A shift of the predominant control frequency to a lower value reflects the existence of debonding defect next to the grout layer. For precast concrete shear walls with the thickness of 20 cm, the above difference may be observed within a distance of 5 cm from the free boundary, beyond which the influence of the free boundary tends to disappear. The results also showed that the fixed boundary of the precast concrete shear wall may lead to higher frequency

responses as compared to the control frequency. In actual construction conditions, the testing response frequencies may vary around the control frequency. The effect of the fixed boundary tends to vanish when the test line is about 15 cm away from the fixed boundary.

6. Recommendations for future study

Despite the effectiveness of the impact-echo test method in detecting the debonding defect in the grout layer of precast concrete shear walls has been validated through the present study, the geometry of the specimens was fixed and the test boundary conditions were ideally defined. In engineering practice, the resonance frequency of the tested panel should be less than the accelerometer's dominant frequency. In the future study, the effect of boundary conditions should be further investigated. Case studies with different wall thicknesses, particularly with more complex field conditions, will be conducted.

Acknowledgements

The authors appreciate the financial support from the National Key Research and Development Program of China (2016YFC0701802, 2016YFC0701507) and Anhui Provincial Natural Science Foundation (KJ2020ZD43, 1908085ME144). In addition, the following companies are gratefully acknowledged for their material donations and assistance to the project: Anhui Hailong Construction Industry Co., LTD, Anhui Institute of Building Research & Design. The first author also wishes to thank the Research Institute for Sustainable Urban Development of Hong Kong Polytechnic University for hosting a 1-year study visit and funding support through a Strategic Focus Area research project (Project code: BBWA).

References

1. Harry R. Foerster; Sami H. Rizkalla; Heuvel, J. Scott. “Behavior and design of shear connections for load bearing wall panels.” *PCI Journal*, Vol. 34, No. 1, 1989, pp. 102-119.
2. P. Choi, D. H. Kim, B. H. Lee, Moon C. Won, “Application of ultrasonic shear-wave tomography to identify horizontal crack or delamination in concrete pavement and bridge.” *Construction and Building Materials*, Vol. 121,2016, pp. 81-91.
3. S.B. Lin, S. Shams, H. Choi, H. Azari, “Ultrasonic imaging of multi-layer concrete structures.” *NDT and E International*, Vol. 98, 2018, pp.101-109.
4. J. K. Zhang, W. Yan, D. M. Cui. “Concrete condition assessment using impact-echo method and extreme learning machines.”. *Sensors*, Vol. 16, No. 4, 2016, pp. 447-464.
5. Mary J. Sansalone, William B. Streett, “Impact-Echo: Nondestructive Testing of Concrete and Masonry.” Bullbrier Press, Jersey Shore, PA, 1997.
6. Nicholas J. Carino, “The impact-echo method: an overview.” *Proc., 2001 Structures Congress and Exposition*, Washington, D.C., National Advances in Nondestructive Testing.12th ed., 2001.
7. Y. Lin, M. Sansalone, “Detecting flaws in concrete beams and columns using the impact-echo method.” *Mater. J Am. Concrete Inst.*, Vol. 89, No. 4, 1992, pp. 394-405.
8. C. Hsiao, C.C. Cheng, T. Liou, Y. Juang, “Detecting flaws in concrete blocks using the impact-echo method.” *NDT & E*. International, Vol. 41, No. 2, 2008, pp. 98-107.
9. Muhammad Tariq A. Chaudhary, "Effectiveness of Impact Echo testing in detecting flaws in prestressed concrete slabs." *Construction & Building Materials*, Vol. No. 10, 2013, pp.753-759.
10. C. T. Hsieh, Y. Lin, “Detecting debonding flaws at the epoxy–concrete interfaces in near-surface mounted CFRP strengthening beams using the impact–echo method.” *NDT & E*. International, Vol. 8, No. 3, 2016, pp. 1-13.
11. Waleed F. Tawhed, Sarah, L. Gassman, “Damage assessment of concrete bridge decks using Impact-Echo method.” *ACI Mater. J* , Vol. 99, No. 3, 2002, pp. 273-81.
12. Y. Lin, K. L. Lin “Transient impact response of bridge I-girders with and without flaws.” *J Bridge Eng. ASCE*, Vol. 2, No. 4, 1997, pp. 131-8.
13. D.G. Aggelis, T. Shiotani, K. Kasai, “Evaluation of grouting in tunnel lining using Impact-Echo.” *Tunn. Undergr. Sp. Tech.*, Vol. 23, No. 6, 2008, pp. 629-37.
14. Mary J. Sansalone, Nicholas J. Carino, “Detecting honeycombing, the depth of surface-opening cracks, and ungrouted ducts using the impact-echo method.” *Concrete Int.*, Vol. 10, No. 4, 1988, pp. 38-46.

15. Nicholas J. Carino, Mary J. Sansalone. “Detecting voids in grouted ducts using the impact-echo method.” *ACI Materials Journal*, Vol. 89, No. 3, 1992, pp. 296-303.
16. Barbara J. Jaeger, Mary J. Sansalone, Randall W. Poston, “Detecting voids in grouted tendon ducts of post-tensioned concrete structures using the Impact Echo Method.” *ACI Struct. J,* Vol. 93, No. 4, 1996, pp. 462-73.
17. Liu, Y.L, Shi J.J., Huang J.Q., Wei G.S. and Wu Z.X., “Grouting defect detection of lapped bar connections based on impact-echo method.” *Shock and Vibration*, Vol. 2009, Article ID 1934240.
18. Lin Y. , Sansalone Mary J., “Transient response of thick rectangular bars subjected to transverse elastic impact.” *J Acous. Soc. Am.,* Vol. 91, No. 5, 1992, pp. 2674-85.
19. Schubert, F., and Köhler, B.. “Ten lectures on impact-echo” *Journal of Nondestructive Evaluation*, Vol.27, No. 1-3, 2008, pp.5-21.
20. Tolstoy, I., and Usdin, E., “Wave propagation in elastic plates: Low and high mode dispersion”, *Journ. of Acoust. Society of Am*., Vol. 29, No. 1, 1957, pp.37–42.
21. Meitzler, A.H., “Backward-wave transmission of stress pulses in elastic cylinders and plates”, *Journ. of Acoust. Society of Am*., Vol.38, 1965, pp.835-842.
22. Gibson, A., and Popovics, J., “Lamb wave basis for impact-echo method analysis”, *J. Eng. Mech-ASCE*, Vol.131, No. 4, 2005, pp. 438-443.
23. Prada, C., Balogun, O., and Murray, T.W., “Laser based ultrasonic generation and detection of zero-group velocity Lamb waves in thin plates”, *Appl. Phys. Lett*., Vol. 87, 2005,194109.
24. Prada, C., Clorennec, D., Royer, D., “Local vibration of an elastic plate and zero-group velocity Lamb modes”, *Journ. of Acoust. Society of Am.,* Vol.124, No. 1, 2008, pp.203–212.
25. Onoe, M., “Contour vibrations of thin rectangular plates”, *Journ. of Acoust. Society of Am*. Vol.30, 1958, pp.1159–1162.
26. Le Clezio E, Predoi M V, Castaings M, et al. “Numerical predictions and experiments on the free-plate edge mode”, *Ultrasonics*, Vol.41, No. 1, 2003, pp. 25-40.
27. Ce`s, M., Clorennec, D., Royer, D., and Prada, C., “Edge resonance and zero group velocity Lamb modes in a free elastic plate”, *Journ. of Acoust. Society of Am.,* Vol.130, No. 2, 2011. pp. 689-694.